special communication

Mathematical models of diffusion-limited gas bubble dynamics in tissue

R. SRINI SRINIVASAN,[1] WAYNE A. GERTH,[2] AND MICHAEL R. POWELL[3]
[1]*Wyle Laboratories, Houston, Texas 77058;* [2]*Department of Anesthesiology, Duke University Medical Center, Durham, North Carolina 27710; and* [3]*Environmental Physiology Laboratory, NASA Johnson Space Center, Houston, Texas 77058*

Srinivasan, R. Srini, Wayne A. Gerth, and Michael R. Powell. Mathematical models of diffusion-limited gas bubble dynamics in tissue. *J. Appl. Physiol.* 86(2): 732–741, 1999.—Mathematical models of bubble evolution in tissue have recently been incorporated into risk functions for predicting the incidence of decompression sickness (DCS) in human subjects after diving and/or flying exposures. Bubble dynamics models suitable for these applications assume the bubble to be either contained in an unstirred tissue (two-region model) or surrounded by a boundary layer within a well-stirred tissue (three-region model). The contrasting premises regarding the bubble-tissue system lead to different expressions for bubble dynamics described in terms of ordinary differential equations. However, the expressions are shown to be structurally similar with differences only in the definitions of certain parameters that can be transformed to make the models equivalent at large tissue volumes. It is also shown that the two-region model is applicable only to bubble evolution in tissues of infinite extent and cannot be readily applied to bubble evolution in finite tissue volumes to simulate how such evolution is influenced by interactions among multiple bubbles in a given tissue. Two-region models that are incorrectly applied in such cases yield results that may be reinterpreted in terms of their three-region model equivalents but only if the parameters in the two-region model transform into consistent values in the three-region model. When such transforms yield inconsistent parameter values for the three-region model, results may be qualitatively correct but are in substantial quantitative error. Obviation of these errors through appropriate use of the different models may improve performance of probabilistic models of DCS occurrence that express DCS risk in terms of simulated in vivo gas and bubble dynamics.

decompression sickness; perfusion; boundary layer

DIFFUSION AND PERFUSION processes thought to govern extravascular gas bubble growth and resolution in tissues have been modeled in terms of ordinary differential equations (ODEs) for various studies of gas bubble behavior in animals and humans. Such models have recently been used in probabilistic treatments of the occurrence of decompression sickness (DCS) in humans (5, 6, 14). These applications entail rigorous determination of model parameter values, such as gas solubilities and diffusivities, that force model behavior into closest possible conformance to observed DCS incidences and times of DCS occurrence in large and heterogeneous "training" data sets. The procedure involved is highly computation intensive and can be undertaken only with bubble dynamics models that can be applied with a minimum of computational overhead to assess DCS risk accumulation during complex pressure and breathing gas profiles.

Bubble dynamics models suitable for these applications fall into one of two classes on the basis of different conceptualizations of the tissue surrounding the gas bubble. In the first model class, the bubble is immersed in a well-stirred tissue compartment but is immediately surrounded by a well-defined boundary layer through which diffusion-limited exchange of gas between bubble and tissue occurs. The model developed by Gernhardt (4) is a typical example of these "three-region" models, which consist of bubble, boundary layer, and tissue regions. In the other model class, the bubble is immersed in an unstirred tissue compartment, and gas exchange between bubble and tissue is limited by bulk diffusion through the tissue. The model developed originally by Van Liew and Hlastala (18) and later elaborated by Hlastala and Van Liew (7), Van Liew (16), and Van Liew and Burkard (2, 17) is typical of these "two-region" models, which consist of only bubble and tissue regions.

Models in either class accommodate the influences of diffusion and surface tension on bubble growth in a physiologically perfused medium and can be readily extended to include effects of tissue elasticity. Their contrasting conceptualizations of the bubble-tissue system yield different equations for the rate of change of bubble radius as a function of time. Although these equations are structurally similar, with differences only in the definitions of certain parameters, the different assumptions under which they are derived impose important limitations on application of the models. Improper application of the models violating these limitations can lead to quantitative model behavior that is inappropriate for the values of the model parameters used. The purpose of this paper is to

The costs of publication of this article were defrayed in part by the payment of page charges. The article must therefore be hereby marked "*advertisement*" in accordance with 18 U.S.C. Section 1734 solely to indicate this fact.

illuminate these issues and their implications in applying the two classes of models to physiological decompression problems.

Glossary

ATA	Atmospheres absolute (1 ATA = 1,013 kPa = 1.013×10^6 dyn/cm^2)
α_b	Solubility of gas in blood (ml gas/ml tissue-ATA)
α_t	Solubility of gas in tissue (ml gas/ml tissue-ATA)
$\alpha_{t,m}$	Solubility of mth diffusible gas in tissue (ml gas/ml tissue-ATA)
λ	Coefficient associated with the sink term of the diffusion equation (μm^{-1}) (1 μm = 10^{-6} m)
σ	Surface tension (dyn/cm)
τ	Tissue time constant (min)
A_i	Bubble surface area (μm^2)
c	Tissue gas concentration (mol/ml)
c_i	Gas concentration at the inner surface of boundary layer (mol/ml)
c_o	Gas concentration at the outer surface of boundary layer (mol/ml)
D_b	Diffusion constant of gas associated with boundary layer (cm^2/min)
D_t	Diffusion constant of gas in tissue (cm^2/min)
$D_{x,m}$	Diffusion constant of mth diffusible gas, in tissue or associated with boundary layer (cm^2/min)
h	Boundary layer thickness (μm)
h_e	"Effective" boundary layer thickness (μm)
j	Number of diffusible gases in tissue
k	Total number of all gases in tissue, including solvent vapor
m, n	Dummy summation indexes
M	Tissue modulus of elasticity (dyn/cm^2/μm^3)
$N_{i,D}$	Molar quantity of all diffusible gases in bubble at the end of each integration step
$N_{i,m}$	Molar quantity of mth diffusible gas in bubble at the end of each integration step
P	Local tissue gas tension (ATA)
P_m	Local tissue gas tension for mth diffusible gas (ATA)
P_a	Arterial gas tension (ATA)
P_v	Venous gas tension (ATA)
P_{amb}	Ambient pressure (ATA)
P_i	Gas pressure in bubble (ATA)
P_t	Tissue gas tension far away from bubble (ATA)
$P_{t,m}$	Tissue tension of mth diffusible gas far away from bubble (ATA)
$P_{i,D}$	Sum of diffusible gas partial pressures in bubble (ATA)
$P_{i,m}$	Partial pressure of mth diffusible gas in bubble (ATA)
$P_{i,n}$	Partial pressure of nth infinitely diffusible gas in bubble (ATA)
$\dot{Q}$	Blood flow per unit volume of tissue (min^{-1})
r	Radial distance from the center of bubble (μm)
r_i	Inner radius of boundary layer (μm)
r_o	Outer radius of boundary layer (μm)
r_∞	Outer radius of tissue (μm)
RT	Product of gas constant and temperature (in units to express solubility in ml gas/ml tissue-ATA)
s	Dummy variable of integration in time (min)
t	Time (min)
Δt	Integration step size (min)
V_i	Bubble volume (μm^3)
V_t	Tissue volume (μm^3)
X	Product of P_iV_i (ATA-μm^3)
$P^0_{i,m}V^0_i$	Initial value of $P_{i,m}V_i$ for mth diffusible gas at each integration step (ATA-μm^3)
$\Delta(P_{i,m}V_i)$	Change in $P_{i,m}V_i$ for mth diffusible gas at each integration step (ATA-μm^3)

BACKGROUND

The basic equations for either model class are the diffusion equation, which describes diffusion of gas through tissue; the Fick equation, which allows calculation of the gas flux through the bubble surface; and the mass balance equation, which determines tissue gas tension. Gases are considered to be ideal. For simplicity, we will neglect solvent vapor pressure and consider cases involving only a single diffusible gas. Generalization of the results to more complex cases is presented in APPENDIX A.

The Diffusion Equation

Neglecting convection due to bubble movement, gas diffusion through the tissue without sources or sinks is described by

$$\frac{\partial c}{\partial t} = D_t \nabla^2 c \qquad (1)$$

where c is concentration of gas in tissue (in moles per unit volume), t is time, and D_t is the bulk diffusion constant of the gas in tissue. Assuming spherical symmetry and denoting the radial distance from the center of the bubble by r, *Eq. 1* becomes

$$\frac{\partial c}{\partial t} = D_t \left(\frac{\partial^2 c}{\partial r^2} + \frac{2}{r} \frac{\partial c}{\partial r} \right) \qquad (2)$$

The Fick Equation

The rate of change of molar concentration of gas in the bubble equals the molar flux of gas through the bubble surface. Thus

$$\frac{1}{RT} \frac{d}{dt} (P_i V_i) = A_i D_t \frac{\partial c}{\partial r} \bigg|_{r=r_i} \qquad (3)$$

where R is the gas constant, T is temperature, P_i is the gas pressure in the bubble, and r_i is the radius of the bubble.[1] $V_i = (4\pi/3) r_i^3$ and $A_i = 4\pi r_i^2$ are the volume and surface area of the bubble, respectively.

Effects of surface tension at the gas-liquid interface of the bubble are incorporated through use of the Laplace equation, which, neglecting tissue viscoelastic effects, is

$$P_i = P_{amb} + 2\sigma / r_i \qquad (4)$$

where P_{amb} is ambient pressure and σ is the gas-liquid surface tension.

[1] Subscript i denotes inner surface and quantities inside the bubble. Subscript o refers to the outer surface of the bubble, when a boundary layer is present.

The Mass Balance Equation

The rate of change of the dissolved gas tension P_t in the tissue at large distances from the bubble is derived from mass balance considerations, assuming equilibration of tissue gas with venous blood gas. The rate of gas uptake by the tissue is the amount carried by the blood per unit time less the flux into the gas bubble. Thus

$$\alpha_t V_t \frac{dP_t}{dt} = \alpha_b V_t \dot{Q}(P_a - P_t) - \frac{1}{RT}\frac{d(P_i V_i)}{dt} \qquad (5a)$$

where $\dot{Q}$ is blood flow per unit tissue volume, P_a is gas partial pressure in arterial blood, V_t is the tissue volume, and α_t and α_b are the gas solubilities in tissue and blood, respectively (in moles per unit volume per unit pressure). For a tissue of infinite volume, division by V_t reduces *Eq. 5a* to

$$\alpha_t \frac{dP_t}{dt} = \alpha_b \dot{Q}(P_a - P_t) \qquad (5b)$$

Note $\alpha_t/(\alpha_b\dot{Q}) = \tau$ is the time constant associated with blood-tissue gas exchange. The tissue half-time is $(\ln 2)\tau$ or 0.693τ.

Equations 2, *3*, and *5* are solved with appropriate boundary conditions to obtain expressions for bubble growth or resolution in tissues according to the presence or absence of gas supersaturation. The equations are coupled and can be solved only numerically. Although numerical solutions are feasible for a given set of parameter values, excessive computational requirements preclude their use in application to DCS studies involving parameter optimization about large training data sets. Therefore, simplifying assumptions are made to obtain expressions of bubble growth that are easier to handle computationally. We examine below simplifications made in the three-region and two-region models to derive ODEs for describing gas bubble dynamics.

Model Descriptions

Three-region model. The three-region model considers the gas bubble to be covered by an unstirred boundary layer of constant and uniform thickness within a well-stirred tissue mass. The uniform gas tension in the tissue outside the boundary layer is determined from *Eq. 5a*, which allows the gas partial pressure in afferent arterial blood to vary with changes in ambient pressure or breathing gas. The concentration gradient across the boundary layer is obtained from *Eq. 2* with the quasi-static approximation[2] (9); that is, by ignoring the time-dependent term $\partial c/\partial t$. Setting $\partial c/\partial t = 0$, the diffusion *Eq. 2* becomes

$$\frac{\partial^2 c}{\partial r^2} + \frac{2}{r}\frac{\partial c}{\partial r} = 0, \qquad r_i \le r \le r_o \qquad (6)$$

where r_i and r_o are the inner and the outer radius, respectively, of the boundary layer around the bubble. *Equation 6* is solved with boundary conditions $c(r_i, t) = c_i$ and $c(r_o, t) = c_o$, to obtain the following expressions for $\partial c/\partial r$

$$\left.\frac{\partial c}{\partial r}\right|_{r=r_i} = (c_o - c_i)\left(\frac{1}{h}\right)\left(\frac{r_o}{r_i}\right) \qquad (7a)$$

$$\left.\frac{\partial c}{\partial r}\right|_{r=r_o} = (c_o - c_i)\left(\frac{1}{h}\right)\left(\frac{r_i}{r_o}\right) \qquad (7b)$$

where $h = (r_o - r_i)$ is the thickness of the boundary layer. Notice that, when multiplied by the appropriate surface areas, these expressions give the same flux through the boundary layer at r_i and r_o. Substituting $r_o = r_i + h$ into *Eq. 7a* yields

$$\left.\frac{\partial c}{\partial r}\right|_{r=r_i} = (c_o - c_i)\left(\frac{1}{h} + \frac{1}{r_i}\right) \qquad (8)$$

To relate concentrations c_i and c_o to pressures, we assume *1*) gas concentrations in the boundary layer follow Henry's law with instantaneous equilibration of gas tensions at r_i and r_o and *2*) same solubility of gas in the boundary layer as in the tissue. Then, we have $c_i = \alpha_t P_i$ and $c_o = \alpha_t P_t$. The desired ODE for the rate of change of bubble radius is obtained from *Eq. 3* by expanding the differential on the left side by using *Eq. 4* (see APPENDIX A), substituting for $\partial c/\partial r$ on the right side using *Eq. 8*, expressing V_i and A_i in terms of r_i, and converting concentrations into partial pressures. We obtain

$$\frac{dr_i}{dt} = \frac{\alpha_t D_b\left(\frac{1}{h} + \frac{1}{r_i}\right)(P_t - P_i) - \frac{r_i}{3}\frac{dP_{amb}}{dt}}{P_{amb} + \frac{4\sigma}{3r_i}} \qquad (9)$$

where D_b is the diffusion constant associated with the boundary layer, which may be different from D_t, the bulk diffusion constant of the gas in tissue. The solubility is expressed in volume units (instead of moles) in *Eq. 9* and thus includes the factor RT from *Eq. 3*. It should be noted that as $h \to \infty$, allowing diffusion through the entire tissue mass, and with constant P_{amb}, *Eq. 9* reduces to the quasi-static form of the solution given by Epstein and Plesset (3) for bubble evolution in isobaric, unperfused media. Also, with no gas flux through the boundary layer ($D_b = 0$), *Eq. 9* reduces to the differential equation for Boyle's law effects on a spherical bubble with surface tension.

With large r_i, the factor $(1/h + 1/r_i)$ in the numerator of *Eq. 9* reduces to $(1/h)$, yielding the expression for dr_i/dt derived by Gernhardt (4) under the assumption that $r_i \cong r_o$. Also, under this assumption, the expressions for the concentration gradients in both *Eqs. 7a* and *7b* reduce to $(c_o - c_i)/h$. *Equation 8* reduces to a similar expression, $(c_o - c_i)/h_e$, without the assumption $r_i \cong r_o$ if we define an "effective" boundary layer

[2] This approximation may not hold during very rapid changes in ambient pressure or breathing gas. In such cases, changes in bubble radius may have to be determined by using the complete diffusion equation.

thickness h_e, which varies as a function of r_i

$$h_e = \left(\frac{1}{h} + \frac{1}{r_i}\right)^{-1} = \frac{hr_i}{h + r_i} \qquad (10)$$

As the bubble enlarges, the effective boundary layer thickness increases asymptotically to the actual thickness h, which remains constant. Such behavior of the effective boundary layer around nitrogen bubbles in water has been observed (13, 15), consistent with the present mathematical formulation.

The three-region model given by *Eq. 9* is a simplification of a more complete solution of *Eq. 2*, including the $\partial c/\partial t$ term, developed by Tikuisis (13). As would be expected, their expression for the concentration gradient derived without the quasi-static approximation is very complex, involving both r and t as independent variables and infinite sums. A simpler formulation similar to that outlined here has also been used by Kunkle (10) to study bubble growth in fluids and by Kunkle and Beckman (11) to calculate bubble dissolution times after recompression.

Two-region model. The bubble in the two-region model lacks a boundary layer and is immersed in an unstirred but uniformly perfused tissue to permit absorption or release of gas by the blood at every point in the tissue. Because the tissue is unstirred, the tissue inert gas tension P is nonuniform and depends on the radial distance r. The effects of perfusion are accommodated by adding a sink (or source) term to *Eq. 2*. In defining this term, the bubble and the tissue, with its embedded sink, must be recognized as the only two regions in the model. Capillaries, with associated arterial and venous gas tensions, are included in the tissue per se and do not explicitly exist. In the absence of bubbles, there is no gas diffusion through the tissue and the tissue gas tension P_t is determined by *Eq. 5b*. The presence of a bubble alters this tension in the vicinity of the bubble, leading to a gas loss or gain that is proportional to the difference between the prevailing local gas tension P and the tissue gas tension P_t that would exist in the absence of the bubble (Fig. 1). The difference is largest at the bubble-tissue interface, and approaches zero far away from the bubble. With the added sink term, *Eq. 2* becomes

$$\alpha_t \frac{\partial P}{\partial t} = \alpha_t D_t \left(\frac{\partial^2 P}{\partial r^2} + \frac{2}{r}\frac{\partial P}{\partial r}\right) - \alpha_b \dot{Q}(P - P_t) \qquad (11a)$$

where tissue gas concentration c has been replaced by $\alpha_t P$. Dividing by $\alpha_t D_t$, we get

$$\frac{1}{D_t}\frac{\partial P}{\partial t} = \frac{\partial^2 P}{\partial r^2} + \frac{2}{r}\frac{\partial P}{\partial r} - \lambda^2(P - P_t) \qquad (11b)$$

where $\lambda^2 = \alpha_b \dot{Q}/\alpha_t D_t = 1/\tau D_t$. Note that the term $\lambda^2(P - P_t)$ acts as a sink if $P > P_t$ and as a source if $P < P_t$.

Equation 11b is solved for the following boundary conditions: $P = P_i$ at $r = r_i$ and $\partial P/\partial r = 0$ as $r \to \infty$. The first condition is the same as in the three-region model. Under the second condition, P_t is defined as the tissue tension too far from the bubble to be influenced by the bubble. Thus it is governed only by perfusion as described by *Eq. 5b*. The solution to *Eq. 11b* is obtained under the quasi-static approximation, i.e., neglecting the time-dependent term $\partial P/\partial t$. The general solution contains both positive and negative exponential terms. However, the positive exponential term vanishes due to the boundary condition at ∞, leading to the following solution at any time, t (18)

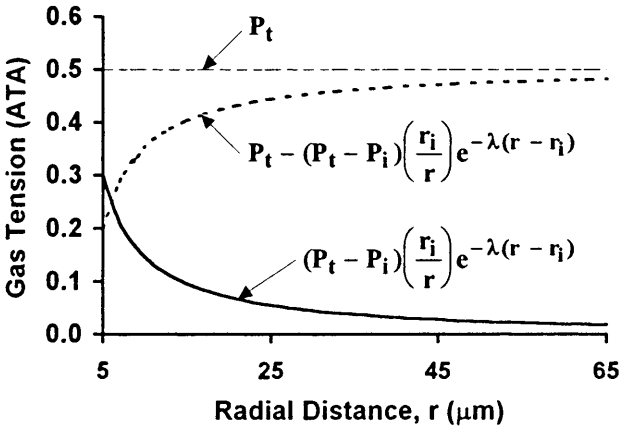

Fig. 1. Solution for two-region model and its components given by *Eq. 12*, showing how diffusion of gas through the tissue affects tissue gas tension in the vicinity of the bubble. All components are slowly varying functions of time, in accord with quasi-static approximation. Diffusion contribution to mass balance is proportional to area under *bottom curve* shown by solid line. Parameter values are as follows: tissue gas tension far away from bubble (P_t) = 0.5 atmospheres absolute (ATA); gas pressure in bubble (P_i) = 0.2 ATA; inner radius of boundary layer (r_i) = 5 μm; coefficient associated with the sink term of the diffusion equation (λ) = 0.004 μm^{-1}.

$$P(r) = P_t - (P_t - P_i)\left(\frac{r_i}{r}\right) e^{-\lambda(r - r_i)}, \qquad r \geq r_i \qquad (12)$$

The pressure gradient at the bubble surface is obtained by differentiating *Eq. 12*

$$\left.\frac{\partial P}{\partial r}\right|_{r=r_i} = (P_t - P_i)\left(\lambda + \frac{1}{r_i}\right) \qquad (13)$$

As before, we expand the differential on the left side of *Eq. 3* by using *Eq. 4*, express V_i and A_i in terms of r_i, and substitute $c = \alpha_t P$ and *Eq. 13* into the result to obtain the following ODE for the rate of change of bubble radius

$$\frac{dr_i}{dt} = \frac{\alpha_t D_t \left(\lambda + \frac{1}{r_i}\right)(P_t - P_i) - \frac{r_i}{3}\frac{dP_{amp}}{dt}}{P_{amb} + \frac{4\sigma}{3r_i}} \qquad (14)$$

Again, the solubility α_t is expressed in volume units to absorb the constant RT. Note that *Eq. 14*, like *Eq. 9* for the three-region model, includes the effects of surface tension and changing hydrostatic pressure (Boyle's law effects) on bubble evolution. With constant P_{amb} and $\dot{Q} = 0$ (and hence $\lambda = 0$), *Eq. 14* also reduces to the

quasi-static form of the expression given by Epstein and Plesset (3) for bubble evolution in isobaric, unperfused media.

Equation 14 differs from the expression originally derived by Van Liew and Hlastala (18) for the two-region model. These workers wrote the diffusion equation with P_a in place of P_t in the sink term and, neglecting the effects of surface tension and changing hydrostatic pressure, obtained a solution under the boundary condition $P = P_a$ as $r \rightarrow \infty$. As a result, their solution differs from our *Eq. 14*, with P_a substituted for P_t, the denominator replaced by P_i (and hence larger by $2\sigma/3r_i$) and no term involving dP_{amb}/dt in the numerator. Recent applications of the two-region model have retained the larger denominator from the original derivation and, hence, do not fully incorporate the effects of surface tension on dr_i/dt (2, 5, 6, 14, 16, 17).

RESULTS

The dynamics of bubble growth after a decompression from sea level to altitude were computed by using each of the models with the parameter values shown in Table 1. Because comparison of model results is meaningful only for large tissue volumes, *Eq. 5b* was used in both cases, i.e., by using *Eqs. 9* and *5b* for the three-region model and *Eqs. 14* and *5b* for the two-region model. The altitude profile consisted of 30 min of 100% oxygen prebreathe at sea-level pressure (1 ATA) followed by ascent at 5,000 ft/min to an indefinitely long residence at 25,000 ft breathing pure oxygen. The diffusion constants D_b and D_t were assumed to be the same. The parameters $\dot{Q}$ and λ were defined to yield a tissue half-time of 360 min.

Table 2 shows the maximum radius and the time to maximum radius of the bubble computed by using the two models for different values of the initial radius. Both the minimum radius for bubble growth and the maximum radius reached are smaller for the two-region model because of the much larger value of $1/\lambda$ (250 μm) relative to h (3 μm). Differences between the two models in the times to attain maximum radius decrease with increasing initial bubble size.

Figure 2 shows the effect of decreasing tissue volume on bubble growth and gas tension P_t in the well-stirred region of the three-region model. For these calculations, bubbles grew from nuclei of 10-μm radius that were assumed to be ever present in the tissue. Bubble growth begins to exert a significant effect on the tissue inert gas tension if the tissue volume does not exceed the maximum bubble volume by more than a factor of $\sim 5 \times 10^4$. With larger tissue volumes, P_t can be computed by using *Eq. 5b* for mass balance with infinite tissue volume rather than the exact *Eq. 5a* for the finite tissue.

Table 1. *Model parameter values used in simulations*

Parameter	Value
Surface tension, σ	30 dyn/cm
Tissue diffusion constant, D_t	1.32×10^{-6} cm^2/min
Boundary layer diffusion constant, D_b	1.32×10^{-6} cm^2/min
Tissue solubility, α_t	0.0125 ml gas/ml tissue-ATA
Blood solubility, α_b	0.0125 ml gas/ml tissue-ATA
Boundary layer thickness, h	3 μm
Tissue half-time, $0.693\ \alpha_t/\alpha_b\ \dot{Q}$	360 min
Blood flow, $\dot{Q}$ (calculated)	0.001925 min^{-1}
Sink coefficient, $\lambda = \sqrt{\alpha_b \dot{Q}/\alpha_t D_t}$	0.004 μm^{-1}
$1/\lambda$	250 μm

Table 2. *Maximum bubble radius and time to maximum radius for the three-region and two-region models obtained by using the parameter values listed in Table 1 and the decompression profile described in the text*

Model	Calculated Variable	Initial Radius, μm			
		r_{min}	15	20	25
Three region (r_{min} = 10.4 μm)*	Maximum radius, r_{max} (μm)	86.3	98.4	106.5	114.1
	Time to r_{max} (min)	384	386	386	387
Two region (r_{min} = 6.3 μm)*	Maximum radius, r_{max} (μm)	19.2	29.2	34.9	40.9
	Time to r_{max} (min)	352	366	369	372

*Minimum radius for bubble growth (r_{min}), below which the bubble spontaneously dissolves.

DISCUSSION

In their original derivation of the two-region model, Van Liew and Hlastala (18) solved the diffusion equation with P_a in place of P_t in the sink term and under the boundary condition $P = P_a$ as $r \rightarrow \infty$. As pointed out by Ball et al. (1), P_a rapidly equilibrates with the inspired gas and is, hence, practically always less than the bubble pressure P_i. The sink term with P_a can thus serve as a physiological source of gas for bubble growth only under extreme and very short-lived conditions. To overcome this problem, Van Liew and Hlastala (18) noted without derivation that P_t could be substituted for P_a in their original solution for dr_i/dt. Contrary to the remarks of Ball et al. (1), we have shown here how this form of the two-region model can be derived directly from the diffusion equation. Our solution also includes the previously neglected effects of surface tension and changing hydrostatic pressure. Hlastala and Van Liew (7) and Meisel et al. (12) also used the boundary condition $P = P_a$ as $r \rightarrow \infty$ in deriving complete solutions to the partial differential equation model including the $\partial P/\partial t$ term in *Eq. 11b*. Their solutions are valid under the same constraint required here [P_a (or P_t) must be independent of r] but also require that P_a be independent of t. Such solutions are, therefore, of limited utility in practical physiological decompression problems.

Unfortunately, neither P_a nor P_t in the definition of the sink term in *Eq. 11a* corresponds to a readily conceptualized physical model. This is because the model implies that a gas tension equal to the chosen value is present everywhere in the tissue. This implication underscores the much larger scale involved in the two-region model compared with that of the three-region model. The two-region model encompasses a very large volume compared with intercapillary dimen-

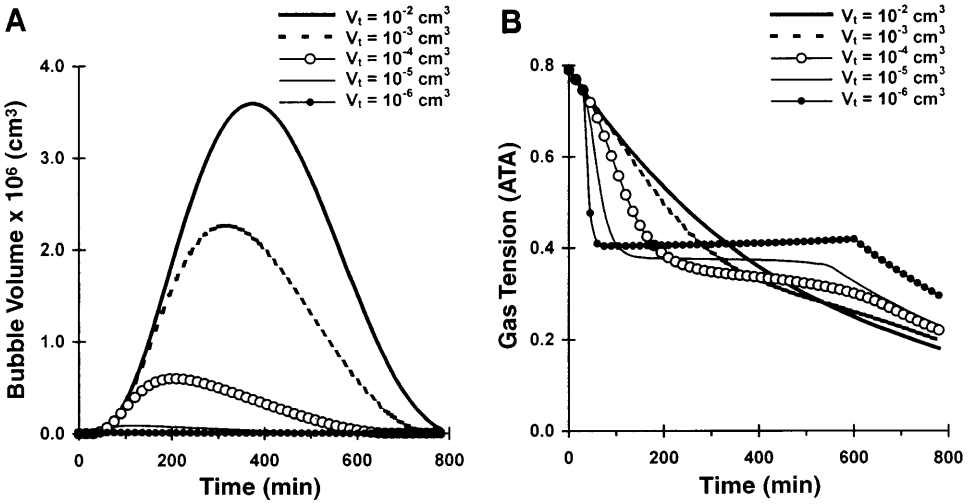

Fig. 2. Effect of tissue volume (V_t) in three-region model on bubble growth (*A*) and inert-gas tension P_t in well-stirred region (*B*) of a 360-min half-time tissue during a 30-min 100% oxygen prebreathe at sea level followed by a 5-min ascent to indefinite exposure at 25,000-ft altitude.

sions, whereas the three-region model encompasses only the volume between nearest-neighbor capillaries. Choice of either P_t or P_a in the definition of the sink term in the two-region model is, therefore, arbitrary but only use of P_t allows consideration of bubble growth with gas washout after decompression.

The two-region model as formulated here is seriously limited by its applicability only to a bubble in a tissue of infinite extent. This limitation and its implications become clear if we examine the nature of the sink for gas diffusing out of the bubble and the maintenance of mass balance in the system. The rate of gas uptake or release by the perfusate at any point in the tissue ($r \geq r_i$) is determined by the blood flow and the local arterial-venous (A-V) gas tension difference and is given by $\alpha_b \dot{Q}(P_a - P_v)$, where P_v is the inert gas partial pressure in venous blood. Under the assumption that gas exchange between tissue and blood is perfusion limited, P_v is equal to the prevailing local tissue tension P. Therefore, the local rate of gas transport due to perfusion is equal to $\alpha_b \dot{Q}(P_a - P)$, which can be expanded as

$$\alpha_b \dot{Q}(P_a - P) = \alpha_b \dot{Q}(P_a - P_t) + \alpha_b \dot{Q}(P_t - P) \quad (15)$$

Substituting for P from *Eq. 12*, we obtain the following expression for the *r* dependence of this transport rate

$$\alpha_b \dot{Q}(P_a - P) = \alpha_b \dot{Q}(P_a - P_t) + \alpha_b \dot{Q}(P_t - P_i)\left(\frac{r_i}{r}\right) e^{-\lambda(r - r_i)}, \qquad r \geq r_i \quad (16)$$

Equation 16 shows how gas transport by perfusion varies in the tissue when it is not well stirred. The A-V difference is dependent on *r*. Tissue-blood gas exchange at all points throughout the tissue includes a position-independent component given by the first term on the right side of *Eq. 16*, which is the same as in *Eq. 5b* for a tissue of infinite extent. As shown in Fig. 1, tissue-blood gas exchange is modified by a diffusion-limited contribution from bubble-tissue gas exchange, which is largest close to the bubble and vanishingly small as $r \rightarrow \infty$. This contribution is given by the second term on the right side of *Eq. 16*, which is seen by comparison to *Eq. 15* to equal the sink term in *Eq. 11a*. All gas losses or gains by the bubble, therefore, occur entirely through the sink term in the diffusion equation. It is erroneous to include an additional accounting for these losses or gains via a $d(P_i V_i)/dt$ term in the ancillary mass-balance equation for P_t. Consequently, *Eq. 5a* cannot be used to incorporate the influence of bubble growth on the tissue dissolved gas tension P_t in the two-region model, while it is appropriately used for this purpose in the three-region model. This analytic property of the three-region model makes it particularly well suited to simulate how dissolved gas depletion by bubble growth influences the evolution of one or more bubbles in a given tissue. Modeling of such interactions in a two-region model is also possible but only by considering the anisotropy of the diffusion field and explicitly solving the gradient equation in all directions around each bubble (8), a process that is too tedious for application in probabilistic models of DCS occurrence.

It is clear by comparing *Eqs. 9* and *14* that a two-region model with given λ and D_t is equivalent to a three-region model with $D_b = D_t$ and $h = 1/\lambda$, provided the tissue volume V_t in the three-region model is sufficiently high to render the $d(P_i V_i)/dt$ term in *Eq. 5a* negligible. Recall $\lambda^2 = 1/\tau D_t$ (see *Eq. 11b*). Because of the reciprocal relationship between *h* and λ, *h* increases with both tissue half-time ($= 0.693\tau$) and diffusion constant D_t ($= D_b$) in equivalent two- and three-region models (Fig. 3). With tissue half-time ranging from 0.36 to 360 min and D_t ranging from 1.3×10^{-8} to 1.3×10^{-3} cm^2/min in a two-region model, the boundary layer thickness in the equivalent three-region model ranges from a fraction of a micrometer to several millimeters.

The high boundary layer volumes corresponding to high values of the boundary layer thickness limit the extent to which results obtained by using certain incorrect implementations of the two-region model can be reconciled by reinterpretation in terms of their corresponding correct three-region model equivalents.

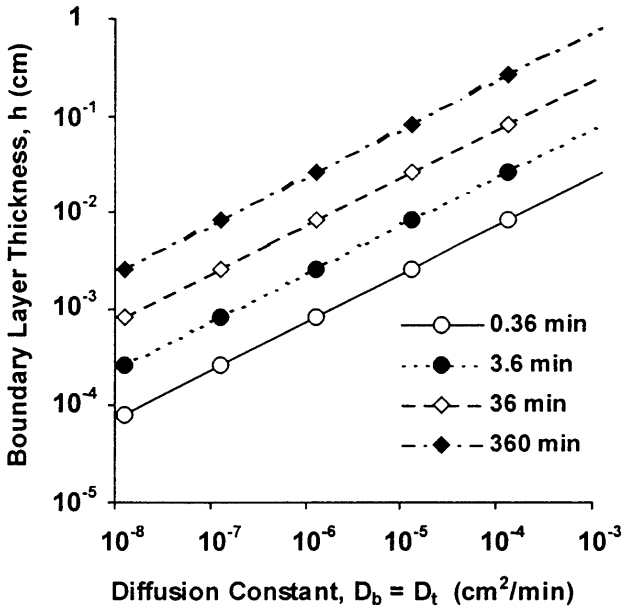

Fig. 3. Dependence of boundary layer thickness on the diffusion constant and compartmental half-time in equivalent two- and three-region models. Note that both axes are logarithmic. D_b, diffusion constant of gas associated with boundary layer; D_t, diffusion constant of gas in tissue.

For example, a two-region model was recently used with *Eq. 5a* to examine how increasing numbers of growing bubbles affect the dissolved gas tensions and maximum bubble volumes in a given volume of supersaturated liquid (17). Such implementations of the two-region model are incorrect but can be viewed as inadvertant applications of the three-region model with $D_b = D_t$, $h = 1/\lambda$, and finite tissue volumes. However, for this reinterpretation to be valid, the parameter values in the two-region model must transform into consistent values of the parameters in the equivalent three-region model. This does not hold for parameters used in the cited work, where bubble growth was considered in tissues with half-times of 5, 40, and 360 min and an assumed $D_t = 0.00132$ cm^2/min (17). Respective values of h in the equivalent three-region model are 0.098, 0.276, and 0.828 cm. These correspond to boundary layer volumes of 0.004, 0.088, and 2.379 cm^3 around bubbles of 2-μm radius, the assumed initial size of the bubbles (17). Because these volumes increase as the bubbles grow from initial size and can never exceed the total liquid volume of the tissue, they are too large to allow consideration of bubble number densities of several hundred or more bubbles per cubic centimeter of liquid, as was attempted. In fact, the boundary layer volume for the initial-size bubble in the 360-min half-time tissue is too large to consider a bubble density as high as 1 bubble/cm^3 liquid. With the assumed value of $D_t = 0.00132$ cm^2/min, dissolved gas depletion by growing bubbles plays only a minimal role at even the highest bubble number densities that can be reasonably considered.

The question remains whether it is possible to obtain acceptable values of h in the equivalent three-region model by altering only the value of the diffusion constant, D_b. At large r_i, dr_i/dt is proportional to D_b/h in the three-region model ($1/h + 1/r_i \cong 1/h$) and to λD_t in the two-region model ($\lambda + 1/r_i \cong \lambda$). Under these conditions, a two-region model with given λD_t is equivalent to a three-region model with $D_b/h = \lambda D_t$, and $V_t \gg$ maximum V_i. Thus lower values of h might be used while retaining near equivalence of the two models if D_b is decreased with respect to D_t ($D_b/D_t < 1$). With $D_b = 1.32 \times 10^{-6}$ cm^2/min ($D_b/D_t = 10^{-3}$), values of h in the 5-, 40-, and 360-min half-time tissues of the equivalent three-region model would be reduced to 0.98, 2.76 and 8.28 μm, respectively. These correspond to respective boundary layer volumes of 7.69×10^{-11}, 4.18×10^{-10} and 4.5×10^{-9} cm^3 around bubbles of 2-μm radius. Even the largest of these volumes would be small enough to consider the influence of as many as 10^5 bubbles/cm^3 of host liquid. However, as illustrated in Fig. 4, the $1/r_i$ term in the expressions for dr_i/dt is not negligible with the conditions and parameter values considered here. Figure 4 shows bubble volume vs. time in a 360-min half-time tissue during the same pressure/respired gas schedule used to generate Fig. 2, as determined by a two-region model and its three-region model equivalent, assuming that $1/r_i$ is negligible and $D_b = D_t \times 10^{-3}$. The tissue volume of 10 cm^3 assumed for the three-region model was sufficiently large to render the $d(P_iV_i)/dt$ term in *Eq. 5a* negligible. The volume-time profiles for the two models would be identical if the $1/r_i$ term contributed negligibly to the time course of bubble evolution in the two models, but this is clearly not the case. The maximum bubble volume achieved in the two-region model is more than three orders of magnitude higher than that achieved in the three-region model. This large difference arises

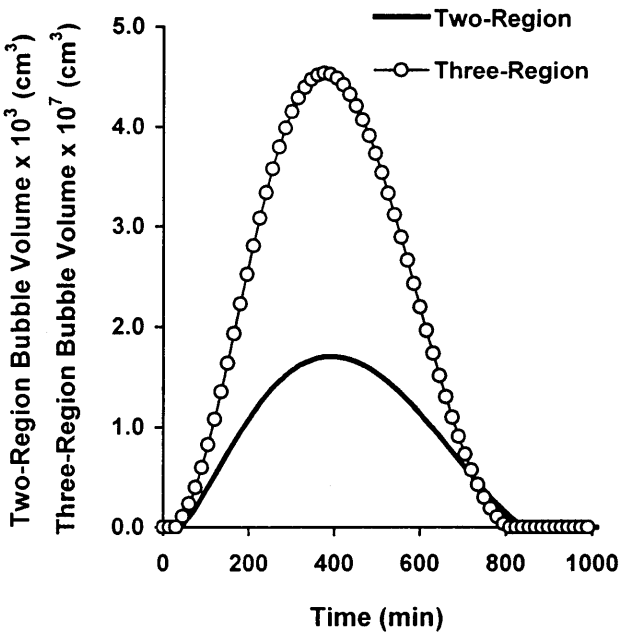

Fig. 4. Bubble volumes as computed by using two-region model and its three-region model equivalent under the assumption of negligible $1/r_i$ and $D_b = D_t \times 10^{-3}$. Note that bubble volume scale for three-region model is four orders of magnitude less than that for two-region model.

from a strong dependence of the solution of the nonlinear differential equation for dr_i/dt on the initial bubble radius when this radius is comparable to h or $1/\lambda$. Thus, when the growth or resolution of the relatively small bubbles that are thought to cause DCS is considered, the equivalence of two- and three-region models at large tissue volumes holds only if $D_b = D_t$. If h assumes inconsistent values under this condition, results obtained from incorrect implementations of the two-region model cannot be quantitatively reconciled with those from properly applied three-region model equivalents.

As illustrated in Fig. 3, two- and three-region models can be formulated that retain equivalence at $V_t \gg$ maximum V_i and with lower values of h across the physiological range of tissue half-times by assuming lower values of $D_b = D_t$. The three-region models of such equivalent pairs can then be exercised by using successively smaller values of V_t to correctly examine the influences of competition between bubbles and blood for dissolved gas. Viewed in this fashion, results from the three-region model for large V_t in Fig. 2 could be modeled by using a two-region model with all parameters but the diffusivity D_t unchanged. Model equivalence in this case requires $D_t = 1.73 \times 10^{-10}$ cm^2/min, or a value more than six orders of magnitude smaller than used in earlier work (17). Because this diffusivity is more than three orders of magnitude smaller than the diffusivity used to obtain the illustrated results, further examination of the influence of decreasing V_t in the three-region model would yield results considerably different from those illustrated. The combination of more reasonable values for D_b and h used to obtain the illustrated results are possible because, unlike in the two-region model, these parameters vary independently of the tissue half-time in the three-region model. Thus, as shown in Fig. 2, essential qualitative features of the interactions between increasing numbers of bubbles in a given tissue volume are evident as described in the above-cited work but at values of the parameters much different from those seemingly allowed with incorrect application of the two-region model.

In summary, the two- and three-region models are structurally similar and can be made equivalent at large tissue volumes through appropriate transformation of certain parameters. Whereas the three-region model can be applied to bubble growth in small tissue volumes, the two-region model is readily applied only to bubble growth in tissues of infinite extent. Two-region models that are incorrectly applied to problems involving bubble growth in finite tissue volumes yield results that may be reinterpreted in terms of their three-region model equivalents, if the parameters in the two-region model transform into consistent values in the three-region model. When such transforms yield inconsistent values for the three-region model, the two-region model results may be qualitatively correct but are in substantial quantitative error. Obviation of these errors through appropriate use of the different models may improve performance of probabilistic models of DCS occurrence that express DCS risk in terms of simulated in vivo gas and bubble dynamics (5, 6).

APPENDIX A

Generalization to Multiple Diffusible Gases

The simplified models presented here are readily generalized to accommodate multiple diffusible gases, tissue viscoelastic effects, and the influences of gases such as water vapor that can be presumed to be always in equilibrium between bubble and surroundings (5). In the following, the term "diffusible gas" will denote a gas with finite diffusivity in the liquid, to distinguish such gases from infinitely diffusible gases that are always in equilibrium between bubble and surroundings. In a mixture of j diffusible gases in $k > j$ gases, with gases $j + 1, j + 2, \ldots, k$ always in equilibrium between bubble and surroundings, the sum of the diffusible gas partial pressures in the bubble, $P_{i,D}$, is given by elaborating *Eq. 4*

$$P_{i,D} = \sum_{m=1}^{j} P_{i,m} = P_{amb} - \sum_{n=j+1}^{k} P_{i,n} + \frac{2\sigma}{r_i} + \frac{4\pi}{3} r_i^3 M \qquad (A1)$$

where the subscript m denotes each of the diffusible gases in the mix, the subscript n denotes the remaining gases, including solvent vapor, and M is the modulus of elasticity for the tissue.

The total flux of diffusible gases across the bubble surface is given as before by the Fick equation

$$\frac{d(P_{i,D}V_i)}{dt} = \sum_{m=1}^{j} \frac{d(P_{i,m}V_i)}{dt} = A_i \sum_{m=1}^{j} \left[\alpha_{t,m} D_{x,m} \left(\frac{dP_m}{dr} \right)_{r=r_i} \right] \qquad (A2)$$

where $\alpha_{t,m}$ is the solubility of diffusible gas m in tissue; $D_{x,m}$ is the diffusivity of diffusible gas m in either the tissue or boundary layer, depending on the model; and $(dP_m/dr)_{r=r_i}$ is the partial pressure gradient of diffusible gas m at the bubble surface.

By expanding the differential on the left side of *Eq. A2* and by using *Eq. A1*, with the assumption that the infinitely diffusible gases remain at constant partial pressure in the bubble, we obtain

$$\begin{aligned} \frac{d(P_{i,D}V_i)}{dt} &= P_{i,D} \frac{dV_i}{dt} + V_i \frac{dP_{i,D}}{dt} \\ &= P_{i,D} A_i \frac{dr_i}{dt} + V_i \left[\frac{dP_{amb}}{dt} + \left(MA_i - \frac{2\sigma}{r_i^2} \right) \frac{dr_i}{dt} \right] \end{aligned} \qquad (A3)$$

By equating the right sides of *Eqs. A2* and *A3*, substituting $V_i = (4\pi/3)r_i^3$ and $A_i = 4\pi r_i^2$, and using *Eq. A1* to replace $P_{i,D}$, we get the following expression for dr_i/dt

$$\frac{dr_i}{dt} = \frac{\sum_{m=1}^{j} \left[\alpha_{t,m} D_{x,m} \left(\frac{dP_m}{dr} \right)_{r=r_i} \right] - \frac{r_i}{3} \frac{dP_{amb}}{dt}}{P_{amb} - \sum_{n=j+1}^{k} P_{i,n} + \frac{4\sigma}{3r_i} + \frac{8\pi}{3} r_i^3 M} \qquad (A4)$$

The change in bubble radius with time is obtained by integrating *Eq. A4* numerically by using the expression for

the partial pressure gradient for each gas at the bubble surface appropriate to the model. For the three-region model, the appropriate expression is given by *Eq. 8* with c, c_i, and c_o replaced by P_m, $P_{i,m}$, and $P_{t,m}$, respectively, where $P_{t,m}$ is the tissue tension for the diffusible gas denoted by *m* as given by *Eq. 5a* or *Eq. 5b* for that gas. For the two-region model, the appropriate expression is given by *Eq. 13*, with P_i and P_t replaced by $P_{i,m}$ and $P_{t,m}$, respectively. In this case, $P_{t,m}$ is given by *Eq. 5b*, as discussed in the text (see DISCUSSION).

The partial pressure of each diffusible gas in the bubble, $P_{i,m}$, at the end of each integration step is computed as follows by using the Dalton's law of partial pressures

$$P_{i,m} = P_{i,D}\left(\frac{N_{i,m}}{N_{i,D}}\right) = P_{i,D}\left\{\frac{P^0_{i,m}V^0_i + \Delta(P_{i,m}V_i)}{\sum_{m=1}^{j}[P^0_{i,m}V^0_i + \Delta(P_{i,m}V_i)]}\right\} \quad (A5)$$

where $N_{i,m}$ is the end-step molar quantity of gas *m* in the bubble, $N_{i,D}$ is the end-step molar quantity of all diffusible gases in the bubble, $P_{i,D}$ is the end-step total diffusible gas partial pressure in the bubble as given by *Eq. A1*. The 0 superscripts of $P_{i,m}$ and V_i denote values at the beginning of the integration step, and $\Delta(P_{i,m}V_i)$ is the change in $P_{i,m}V_i$ product over the integration interval, obtained by integrating *Eq. A2*.

Equation A4 provides a comprehensive description of bubble dynamics for either a two-region or a three-region model, including the effects of bubble-tissue gas fluxes, surface tension, tissue elasticity, and changes in ambient hydrostatic pressure (Boyle's law effects). The two-region model version of this equation differs from that described by Burkard and Van Liew (2), because they used an expression for dr_i/dt based on the original single-gas derivation (18) in which effects of surface tension, tissue elasticity, and changing hydrostatic pressure were neglected. Their separate equation for Boyle's law effects with iterative approximation to find V_i and $P_{i,m}$ in each time step (2) is not required with the present formulation.

APPENDIX B

Mass Balance in the Three-Region Model With a Finite Tissue Volume

We assume that there is no gas exchange or blood flow in the boundary layer region and that the tissue volume including the boundary layer remains constant. Expressing the rate of change of gas content in moles per unit time, we have

$$\text{Rate of change of bubble gas content} = (1/RT)\frac{d}{dt}(P_iV_i)$$

where P_i is the bubble pressure given by *Eq. 4*, and V_i is the bubble volume

$$\text{Rate of change of tissue gas content} = \frac{d}{dt}\int_{r_o}^{r_\infty}\alpha_t P(r,t)4\pi r^2 dr$$

where r_∞ is the outer radius of a spherically shaped tissue, and

$$\text{Rate of gas transport by perfusion} = \int_{r_o}^{r_\infty}\alpha_b\dot{Q}[P_a - P(r,t)]4\pi r^2 dr$$

Mass balance implies that, in any given time interval, the sum of changes in bubble and tissue gas contents equals the amout of gas transported by perfusion. Therefore

$$\frac{d}{dt}(P_iV_i) + \frac{d}{dt}\int_{r_o}^{r_\infty}\alpha_t P(r,t)4\pi r^2 dr = \int_{r_o}^{r_\infty}\alpha_b\dot{Q}[P_a - P(r,t)]4\pi r^2 dr \quad (B1)$$

where the solubilities α_t and α_b are expressed in appropriate units to include the factor RT. With α_t thus expressed, we use $V_i = (4\pi/3)r_i^3$ and *Eqs. 4* and *9* to obtain

$$\frac{d}{dt}(P_iV_i) = 4\pi r_i^2\left[\alpha_t D_b\left(\frac{1}{h} + \frac{1}{r_i}\right)(P_t - P_i)\right] \quad (B2)$$

Also, $P(r,t) = P_t(t)$, independent of *r*, and therefore

$$\int_{r_o}^{r_\infty}\alpha_t P(r,t)4\pi r^2 dr = \alpha_t P_t\frac{4\pi}{3}(r_\infty^3 - r_o^3) = \alpha_t P_t(V_t + V_i - V_o) \quad (B3)$$

where $V_o = (4\pi/3)r_o^3$ is the volume of the bubble including the boundary layer. V_t is the total volume of tissue including the boundary layer region. Note that the tissue need not be spherical in shape; in other words, the outer radius r_∞ is irrelevant. Using *Eq. B3*, we obtain

$$\frac{d}{dt}\int_{r_o}^{r_\infty}\alpha_t P(r,t)4\pi r^2 dr = \alpha_t(V_t + V_i - V_o)\frac{dP_t}{dt} - \alpha_t P_t 4\pi(r_o^2 - r_i^2)\frac{dr_i}{dt} \quad (B4)$$

$$\int_{r_o}^{r_\infty}\alpha_b\dot{Q}[P_a - P(r,t)]4\pi r^2 dr = \alpha_b\dot{Q}(P_a - P_t)(V_t + V_i - V_o) \quad (B5)$$

Equating the right sides of *Eqs. B2* and *B4* to the right side of *Eq. B5* (according to *Eq. B1*) yields the following mass balance equation for the three-region model

$$\frac{dP_t}{dt} = \frac{P_a - P_t}{\tau} - \frac{4\pi}{(V_t + V_i - V_o)}\times\left[D_b\left(\frac{1}{h} + \frac{1}{r_i}\right)(P_t - P_i)r_i^2 - P_t(r_o^2 - r_i^2)\frac{dr_i}{dt}\right] \quad (B6)$$

The first term within brackets on the right side of the above equation is due to gas flux through the bubble surface given by *Eq. B2*. This term is the same as the last term on the right side of *Eq. 5a*, except for the solubility factor α_t (including the factor RT), which is canceled out by division. The second term within brackets involving dr_i/dt arises by differentiating $(V_i - V_o)$ and substituting $dr_o/dt = dr_i/dt$ (see *Eq. B4*). Our simulation results indicate that this term does not significantly change the maximum bubble radius (<0.33% by using the parameter values shown in Table 1 and a tissue volume of 10^{-6} cm^3) and can, therefore, be ignored. Note that as $V_t \rightarrow \infty$, the terms in brackets vanish, and *Eq. B6* reduces to *Eq. 5b*.

For a given decompression profile, the time course of changes in bubble radius is determined by solving *Eqs. 9* and *B6* simultaneously. We derive below another form of *Eq. B6* that requires slightly less computations in each integration step by solving the mass balance equation with some approximations. Ignoring the small difference $(V_i - V_o)$, $(V_t + V_i - V_o) \approx V_t$. Then, with use of *Eq. B3*, *Eq. B1* becomes

$$\frac{dP_t}{dt} + \frac{P_t}{\tau} = \frac{P_a}{\tau} - \frac{1}{\alpha_t V_t}\frac{dX}{dt} \qquad (B7)$$

where $X = P_i V_i$.

Multiplying both sides of *Eq. B7* by $e^{t/\tau}$ (integrating factor) and integrating between t and $t + \Delta t$, we obtain

$$P_t(t+\Delta t)e^{(t+\Delta t)/\tau} - P_t(t)e^{t/\tau} = P_a[e^{(t+\Delta t)/\tau} - e^{t/\tau}] - \frac{1}{\alpha_t V_t}\int_t^{t+\Delta t} e^{s/\tau}\left.\frac{dX}{dt}\right|_s ds \qquad (B8)$$

where Δt is the integration step size and s is the dummy variable of integration.

The integral in *Eq. B8* above can be evaluated by approximating $X(s)$ by a straight line in the interval $[t, t + \Delta t]$, i.e., by letting $X(s) = X(t) + [X(t + \Delta t) - X(t)/\Delta t](s - t)$ for $t \leq s \leq t + \Delta t$. Simplifying the result, we get the following expression for tissue tension at time $(t + \Delta t)$

$$P_t(t+\Delta t) = P_t(t) + \left[P_a - P_t(t) - \frac{X(t+\Delta t) - X(t)}{\alpha_t V_t}\frac{\tau}{\Delta t}\right](1 - e^{-\Delta t/\tau}) \qquad (B9)$$

Note that as $V_t \rightarrow \infty$, the last term within brackets on the right side of the above equation becomes 0, and the solution reduces to that of *Eq. 5b*. In applying *Eq. B9*, we first solve *Eq. 9* for r_i assuming P_t to be constant in the interval $[t, t + \Delta t]$, in accord with the quasi-static approximation. We then use *Eq. B9* to update P_t. Thus *Eq. B9* needs to be used only once during each integration step. Also, it should be noted that expressions similar to *Eq. B9* for $P_t(t + \Delta t)$ can be derived using other approximations for $X(s)$ in the interval $(t, t + \Delta t)$ (e.g., exponential).

The authors gratefully acknowledge Dr. Edward D. Thalmann and Dr. Richard D. Vann for critical reviews of this manuscript.

This work was supported in part by National Aeronautics and Space Administration Cooperative Agreement NCC 9-42 and US Navy contract N0463A-97-M-0126 (to W. A. Gerth).

Address for reprint requests: R. Srini Srinivasan, Wyle Laboratories, 1290 Hercules Dr., Suite 120, Houston, TX 77058-2769.

Received 22 January; accepted in final form 23 September 1998.

REFERENCES

1. **Ball, R., J. Himm, L. D. Homer, and E. D. Thalmann.** Does the time course of bubble evolution explain decompression sickness risk? *Undersea Hyperb. Med.* 22: 263–280, 1995.
2. **Burkard, M. E., and H. D. Van Liew.** Simulation of exchanges of multiple gases in bubbles in the body. *Respir. Physiol.* 95: 131–145, 1993.
3. **Epstein, P. S., and M. S. Plesset.** On the stability of gas bubbles in liquid-gas solutions. *J. Chem. Phys.* 18: 1505–1509, 1950.
4. **Gernhardt, M. L.** *Development and Evaluation of a Decompression Stress Index Based on Tissue Bubble Dynamics.* (PhD dissertation). Philadelphia: Univ. of Pennsylvania Press, 1991.
5. **Gerth, W. A., and R. D. Vann.** *Development of Iso-DCS Risk Air and Nitrox Decompression Tables Using Statistical Bubble Dynamics Models.* Bethesda, MD: Office of Undersea Research, 1996. (Final Rep. Contract NA46RU0505, National Oceanic and Atmospheric Administration)
6. **Gerth, W. A., and R. D. Vann.** Probabilistic gas and bubble dynamics models of DCS occurrence in air and N_2O_2 diving. *Undersea Hyperb. Med.* 24: 275–292, 1997.
7. **Hlastala, M. P., and H. D. Van Liew.** Absorption of in vivo inert gas bubbles. *Respir. Physiol.* 24: 147–158, 1975.
8. **Jiang, Y., L. D. Homer, and E. D. Thalmann.** Development and interactions of two inert gas bubbles during decompression. *Undersea Hyperb. Med.* 23: 131–140, 1996.
9. **Keller, J. B.** Growth and decay of gas bubbles in liquids. In: *Proceedings of the Symposium on Cavitation in Real Liquids*, edited by R. Davies. New York: Elsevier, 1964, p. 20–29.
10. **Kunkle, T. D.** *Bubble Nucleation in Supersaturated Fluids.* Honolulu: Univ. of Hawaii at Manoa Press, 1979. (University of Hawaii Sea Grant Tech. Rep. UNIHI-SEAGRANT-TR-80-01)
11. **Kunkle, T. D., and E. L. Beckman.** Bubble dissolution physics and the treatment of decompression sickness. *Med. Phys.* 10: 184–190, 1983.
12. **Meisel, S., A. Nir, and D. Kerem.** Bubble dynamics in perfused tissue undergoing decompression. *Respir. Physiol.* 43: 89–98, 1981.
13. **Tikuisis, P.** *The Stability and Evolution of a Gas Bubble in a Finite Volume of Stirred Liquid* (PhD dissertation). Ontario, Canada: Univ. of Toronto Press, 1981.
14. **Tikuisis, P., K. A. Gault, and R. Y. Nishi.** Prediction of decompression illness using bubble models. *Undersea Hyperb. Med.* 21: 129–143, 1994.
15. **Tikuisis, P., C. A. Ward, and R. D. Venter.** Bubble evolution in a stirred volume of liquid closed to mass transport. *J. Appl. Physiol.* 54: 1–9, 1982.
16. **Van Liew, H. D.** Simulation of the dynamics of decompression sickness bubbles and the generation of new bubbles. *Undersea Hyperb. Med.* 18: 333–345, 1991.
17. **Van Liew, H. D., and M. E. Burkard.** Density of decompression bubbles and competition for gas among bubbles, tissue, and blood. *J. Appl. Physiol.* 75: 2293–2301, 1993.
18. **Van Liew, H. D., and M. P. Hlastala.** Influence of bubble size and blood perfusion on absorption of gas bubbles in tissues. *Respir. Physiol.* 7: 111–121, 1969.